JOURNAL OF CATALYSIS 129, 426–437 (1991)

# A Study of Catalytic Activity, Constituent, and Structure of V–Ag Catalyst for Selective Oxidation of Toluene to Benzaldehyde

ZHANG HUI-LIANG,[1] ZHONG WEI, DUAN XIANG, AND FU XIAN-CAI

*Department of Chemistry, Nanjing University, Nanjing, 210008, People's Republic of China*

Received October 18, 1989; revised January 3, 1991

A series of V–Ag mixed oxide catalysts with various atomic ratios of V and Ag were prepared by a solution-mixing method. XRD, TEM, SMEA (surface micro-area element analysis), ESR, FT–IR, etc., were used to study the physicochemical properties of the catalysts. The experimental results showed that when silver was introduced into the vanadium pentoxide, the V=0 bond was weakened, and the specific activity of the sample increased. When the atomic ratios of V/Ag were set between 3/1 and 1/1, the selectivity for benzaldehyde increased. In particular, when the V/Ag ratio equaled 2.16, the selectivity for benzaldehyde was greatest, the absorption peak of 900 $cm^{-1}$ in FT–IR shifted to lower energy, and the relative quantity of $V^{4+}$ measured with ESR appeared the highest. After reaction, XRD showed the main phases of the catalyst to exist as $Ag_{0.80}V_2O_5$, and $Ag_{0.68}V_2O_5$, with a minor Ag phase. Small amounts of $VO_2$ and $V_2O_4$ were also detected. On the two component oxides of vanadium–silver, the toluene oxidation appeared to proceed through two parallel reaction paths: side-chain oxidation of toluene and oxidative coupling. The sample of pure silver promoted cleavage of the carbon ring of toluene and produced deep-oxidation products in large quantity, while the sample of pure $V_2O_5$ promoted the oxidative coupling of toluene. After the addition of silver to $V_2O_5$, however, the oxidative coupling reaction was depressed, and the silver–vanadium oxide phases, $Ag_{0.80}V_2O_5$ and $Ag_{0.68}V_2O_5$, were formed. These two phases are responsible for the selective oxidation of toluene. 

## INTRODUCTION

The subject of selective oxidation of toluene to benzaldehyde with $MoO_3$- and $V_2O_5$-based catalysts in the presence of air has been extensively studied in the past 15 years. For example, the investigation of bismuth molybdate and various molybdenum-containing catalysts used for this reaction have been reported (*1–3*). Both supported and unsupported Fe–Mo oxides have been studied for finding a practical catalyst, and for understanding the relationship between the catalytic activity and the physicochemical properties of the catalyst (*4–7*). Three especially interesting studies have been performed, one by Jonson *et al.* (*8*) using $V_2O_5/\gamma$-$Al_2O_3$ with different vanadium loadings, another by Mori *et al.* (*9*) adopting well-characterized $V_2O_5$ for toluene oxidation, and a third by Jonson *et al.* (*10*) who have related the rate of the selective oxidation of toluene to the frequencies of the metal oxide ion vibrations. In addition, the reports about the catalysts such as $V_2O_5$–$K_2SO_4/SiO_2$ (*11*), V–Mo–Ce oxide (*12*), $V_2O_5$–$SnO_2$ (*13, 14*), V–Ag oxide, and Ag–Ce–vanadate (*15–18*), which contained vanadium as a main constituent and exhibited a good performance for the selective oxidation of toluene, have often appeared in the literature. Considering the two-component catalysts, some authors (*16, 17*) suggest that the V–Ag oxide for the selective oxidation of toluene to benzaldehyde is good. The catalyst has usually been prepared by a fusion of $V_2O_5$ (or $NH_4VO_3$) and $Ag_2O$ (or $AgNO_3$), and its composition is quite complex. Casalot and Pouchard (*19*) have studied the V–Ag oxide with the $V_2O_5/Ag_2O$ mole ratios from 1 to 19, and showed that four different V–Ag compounds existed in the samples. Except

[1] To whom correspondence should be addressed.



0021-9517/91 $3.00

for Ref. (*17*), which reported the effect of the structure and acid–base properties of V–Ag catalyst on the selective oxidation of toluene, very few reports on this subject have been found so far. In order to explore the influence of different preparation methods on the physicochemical properties, the constituents, the structure of catalysts, and thus the selective oxidative reaction to toluene, we have prepared a series of V–Ag catalysts with various V/Ag atomic ratios using the rather simple solution-mixing method. Various analytical techniques, such as XRD, FT–IR, ESR, TEM, SMEA (surface micro-area element analysis), have been used for characterization.

## EXPERIMENTAL

*1. Sample preparation.* According to a certain proportion of vanadium and silver desired, the silver nitrate aqueous solution was added to the ammonium *meta*-vanadate aqueous solution (in which the oxalic acid was also added to promote dissolution) with constant stirring. The formed suspended mixture in liquid was placed in a circulating film-evaporator to evaporate. The dried mass was calcined in a muffle furnace at 723 K for 9 hr, and then these materials were pelleted, crushed, and sieved.

*2. Catalytic activity measurements.* The catalytic activity measurements were carried out in a flowing system by using a quartz reaction tube (inside diameter 20 mm). The catalyst loading was 0.500 g of granules in the size range of 20–40 mesh. These were diluted with 3 ml quartz sand of the same size. The space velocity was 8900 ml $\cdot$ $h^{-1}$ $\cdot$ $g^{-1}$, air/toluene mole ratio was 5, and the bed temperature was 673 K. The $CO_x$ was measured with an Orsat gas apparatus. The liquid product was collected at liquid nitrogen temperature and was measured by using the gas chromatograph method with the xylene as the internal standard.

*3. XRD analysis.* The XRD was performed with a Rigaku D/Max-RA X-ray diffractometer using a Cu target and a graphite monochromator, with an applied voltage of 30 kV and a current of 50 mA.

*4. FT–IR spectra measurements.* The samples were mixed with KBr and then pelleted. The spectra were recorded in Nicolet 5DX FT–IR spectrometer over the range 1400–400 $cm^{-1}$.

*5. Specific surface area measurements.* The specific surface area was measured with the aid of a Beijing ST-03 Type porosity/specific surface instrument using a single gas path. Helium was used as the carrier gas. The desorption peak area of $N_2$ was recorded on Shanghai CDMA-IA chromatographic data treater, and the BET formula was used to obtain the results of specific surface area.

*6. TEM and SMEA measurements.* An aqueous suspension of samples was dispersed by ultrasonication, and then was dropped on a copper gauze covering with collodion. The measurements were carried out in JEOL JEM-200CX electron microscope. The SMEA measurements of partial samples were performed with a JEM-200CX, 860-500 micro-area analyzer system.

*7. ESR measurements.* ESR spectra were recorded on a Brucker ER 200-D-SRC 10/12 spectrometer. The relative quantitative results of the ESR signal were obtained by performing the second integration with an ASPECJ 3000 computer.

## RESULTS AND DISCUSSION

### *1. Catalytic Activity*

The vapor-phase catalytic oxidation of toluene has three reaction paths: (i) side-chain oxidation, (ii) oxidative coupling reaction, and (iii) direct oxidation of the aromatic ring. These reactions can produce 23 kinds of products (*20*). The results of the catalytic activity for toluene oxidation and the specific surface area of the V–Ag series samples are given in Table 1. From this table, it is observed that after the silver was added to vanadium pentoxide, the conver-

TABLE 1

Catalytic Activity and Specific Surface Area of Different V–Ag Samples

| Sample number | V/Ag (atomic ratio) | Conversion of toluene (mol%) | Selectivity for $C_6H_5CHO$ (mol%) | Selectivity for $CO_x$ (mol%) | Specific surface area ($m^2/g$) | Specific activity (m mol/ $h^1 \cdot m^2$) |
|---|---|---|---|---|---|---|
| Y-1 | 1/0 | 22.8 | 6.1 | 18.8 | 3.14 | 0.98 |
| Y-2 | 9/1 | 30.4 | 9.5 | 18.6 | 3.51 | 1.17 |
| Y-3 | 3/1 | 25.8 | 21.7 | 18.3 | 1.23 | 2.82 |
| Y-4 | 2.16/1 | 14.8 | 57.0 | 17.2 | 0.64 | 3.11 |
| Y-5 | 1.5/1 | 24.5 | 26.5 | 20.6 | 0.86 | 3.83 |
| Y-6 | 1/1 | 27.0 | 22.1 | 22.9 | 0.49 | 7.42 |
| Y-7 | 0/1 | 14.0 | 0.0 | 90.1 | 0.20 | 9.42 |

sion of toluene increased at first, but with the further addition of silver, the conversion of toluene decreased and approached a minimum value of 14.8% and then increased again. However, following the increase of the silver content in samples, the selectivity of benzaldehyde was also increased, until it achieved a maximum value of 57.0%, and then began to decrease. Moreover, the increase in specific activities of samples followed the increase of silver content, and the specific activity of the pure silver sample (Y-7) was the largest; this result is contrary to the report in Ref. (*17*). In addition, it is observed that following the increase of silver content, the oxidative coupling products of reaction in the experiment, viz., methyldiphenyl methane, anthraquinone, were decreased, too.

### 2. *The Characterization of Catalyst Structure*

(i) *Results of XRD.* XRD results of catalysts before and after reaction are given respectively in Tables 2 and 3. The Y-1 sample (V/Ag = 1/0) was prepared by decomposition of $NH_4VO_3$ under a large flow of air at 723 K for 9 hr. The results of XRD showed that the phase of Sample Y-1 before reaction was $V_2O_5$, and after reaction it was transformed to $V_4O_9$ and $VO_2$, while a very small amount of unreduced $V_2O_5$ remained.

The Y-2 sample (V/Ag = 9/1) before reaction contained $AgV_7O_{18}$ and $Ag_{0.35}V_2O_5\beta$, and a small amount of $V_2O_5$. After reaction the phases which existed in Sample Y-2 were $V_2O_4$, $VO_2$, and elemental silver, but phases of silver–vanadium compounds were not detected in this sample.

In Sample Y-3 (V/Ag = 3–1) before reaction, the $V_2O_5$ phase disappeared as compared with the Samples Y-1 and Y-2. Aside from the small amount of $AgV_7O_{10}$ and $Ag_{0.35}V_2O_5\beta$ phase, a new silver–vanadium oxide phase $Ag_{1.2}V_3O_8$ occurred. When the silver content in samples increased continuously to V/Ag = 2.16, i.e., Sample Y-4, the existing phases were merely the silver–vanadium oxide phases, $Ag_2V_4O_{10.84}$ and $Ag_{1.2}V_3O_8$. In Samples Y-5 and Y-6 the phases occurring were $Ag_2V_4O_{10.84}$ and $AgVO_3$, with a very minor silver phase occurring in Sample Y-6. For samples from Y-3 to Y-6 after reaction, various amounts of silver–vanadium oxide phases, $Ag_{0.80}V_2O_5$ and $Ag_{0.68}V_2O_5$, and elemental silver existed. In Table 1, it is shown that the selectivities for benzaldehyde over the four samples (Y-3 to Y-6) were obviously high (>20%). The relative amount of the silver–vanadium oxide phase in Sample Y-4 (V/Ag = 2.16) was the largest and that of silver was the least. This sample also has the highest selectivity for benzaldehyde (Table 1). According to the references (*21, 22*), $V_2O_4$ is an inactive phase in ammoxidative

TABLE 2

Results of XRD Analysis of Different V–Ag Samples before Reaction

| Sample number | $V_2O_5$ | $AgV_7O_{18}$ | $Ag_{0.35}V_2O_5\beta$ | $Ag_{1.2}V_3O_8$ | $Ag_2V_4O_{10.84}$ | $AgVO_3$ | Ag |
|---|---|---|---|---|---|---|---|
| Y-1 | VS | | | | | | |
| Y-2 | M | S | S | | | | |
| Y-3 | | W | W | VS | | | |
| Y-4 | | | | S | VS | | |
| Y-5 | | | | | M | S | |
| Y-6 | | | | | W | VS | VW |
| Y-7 | | | | | | | VS |

*Note.* (S) strong, (M) medium, (W) weak, (V) very.

oxidation. Thus it appears that silver–vanadium oxide phases are responsible for the oxidation reaction of toluene to benzaldehyde. This point of view was supported by the results from Ref. (*17*).

(ii) *FT–IR measured results.* Figures 1 and 2 are the FT–IR spectra of V–Ag series samples before and after reaction, respectively. For Sample Y-1 before reaction, the absorption peak at 1021 $cm^{-1}$ is assigned to the $(V{=}O)^{3+}$ stretching vibration (*23, 24*), and the absorption peak of 827 and 614 $cm^{-1}$ to the asymmetry and symmetry stretching virbration of V–O–V units having a bridged and a 2-coordinated oxygen species (*25*), respectively; the absorption peak at 478 $cm^{-1}$ was referred to lattice vibration (*24*) or V–O–V rotational vibration (26). In Sample Y-1 after reaction (see Fig. 2), the absorption peak at 1021 $cm^{-1}$, which belongs to $(V{=}O)^{3+}$ stretching vibration, clearly weakened, and a new peak at 980 $cm^{-1}$ occurred, which might be assigned to $(V{=}O)^{2+}$ stretching vibration (*27*).

The FT–IR spectrum of Sample Y-2 (V/Ag = 9/1) before reaction (Fig. 1) shows that the addition of silver caused the absorption peak of $(V{=}O)^{3+}$ stretching vibration to shift from 1021 to 1001 $cm^{-1}$. However, for the V–Ti–O catalyst, Andersson (*28*) also obtained the same result (i.e., a red shift occurred from 1023 to 995 $cm^{-1}$) and suggested that this shift may be due to the presence of a number of disordered vacancies in the $V_2O_5$ lattice and can be related to a decrease of $P_\pi - d_\pi$ oxygen–metal interaction and an increased electrostatic repulsion of the vanadium and oxygen species, as illustrated in Fig. 3. In addition, two new absorption peaks occurred at 984 and 933

TABLE 3

Results of XRD Analysis of Different V–Ag Samples after Reaction

| Sample number | $V_2O_5$ | $V_4O_9$ | $VO_2$ | $V_2O_4$ | Ag | $Ag_{0.80}V_2O_5$ | $Ag_{0.68}V_2O_5$ |
|---|---|---|---|---|---|---|---|
| Y-1 | VW | S | S | | | | |
| Y-2 | | | S | S | S | | |
| Y-3 | | | W | M | S | M | M |
| Y-4 | | | W | W | M | S | S |
| Y-5 | | | M | M | VS | M | M |
| Y-6 | | | M | M | VS | M | M |
| Y-7 | | | | | VS | | |

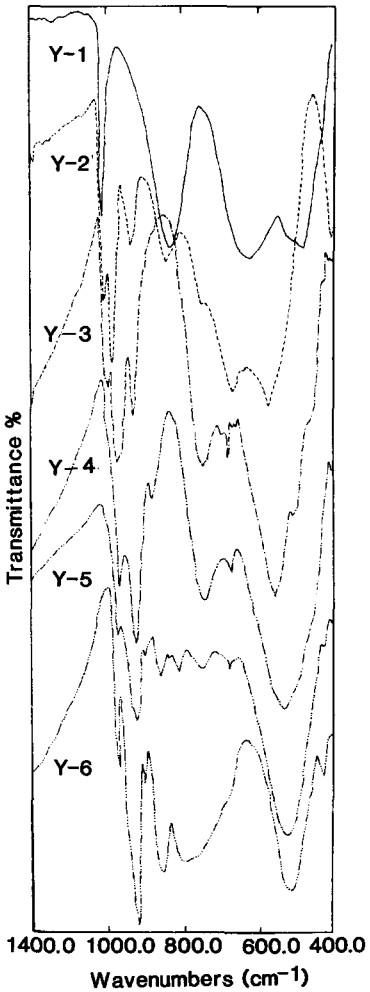


FIG. 1. FT–IR spectra of V–Ag samples before reaction.

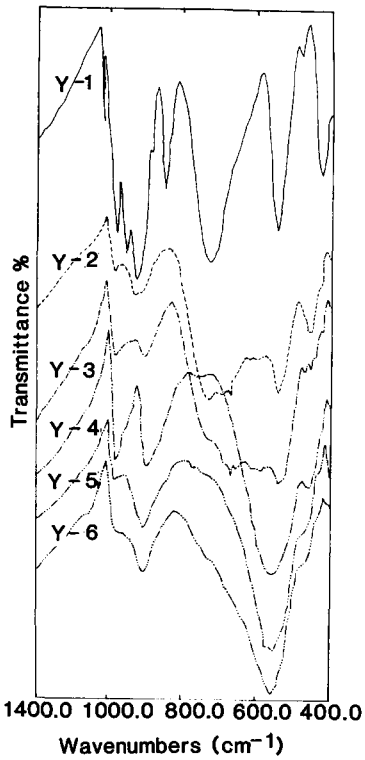


FIG. 2. FT–IR spectra of V–Ag samples after reaction.

$cm^{-1}$, respectively. The adsorption peak of 984 $cm^{-1}$ could be assigned to $(V{=}0)^{2+}$ stretching vibrations (*27*), and it was consistent with the appearance of $V^{4+}$ signal in the subsequent ESR measurement.

As the silver content in Samples Y-3 to Y-6 before reaction increased, a red shift was observed, i.e., the absorption peak at 933 $cm^{-1}$ moved toward 920 $cm^{-1}$ and the absorption peak at 984 $cm^{-1}$ moved to 965 $cm^{-1}$. Barraclough *et al.* (*29*) reported that those absorption bands in the range of 900–1100 $cm^{-1}$ should be assigned to the stretching vibration of metal–oxygen double bond (Me=O).Considering the results of XRD in Table 2, the existing absorption peaks at 984 and 933 $cm^{-1}$ could be assigned to the formation of the silver–vanadium oxide phases. Because of the substitution of $Ag^{+}$ ion for some $V^{5+}$ or $V^{4+}$ ions in the lattice of these new phases, the bond of V=O was weakened. After reaction, the absorption peaks changed a little and two rather strong absorption bands occurred at about 980 and 900 $cm^{-1}$ (Fig. 2, the spectra

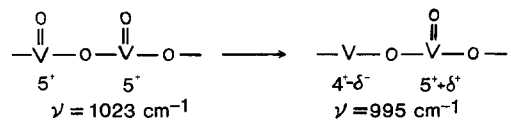


FIG. 3. Schematic presentation of the electrostatic repulsion of the vanadium and oxygen species in the $V_2O_5$ lattice.

TABLE 4

Results of ESR Analysis of Different V–Ag Samples after Reaction

| Sample number | Y-1 | Y-2 | Y-3 | Y-4 | Y-5 | Y-6 |
|---|---|---|---|---|---|---|
| V/Ag (Atomic ratio) | 1/0 | 9/1 | 3/1 | 2.16/1 | 1.5/1 | 1/1 |
| Peak area/g | 0.73 | 2.35 | 2.55 | 3.93 | 3.20 | 3.06 |

of Sample Y-3 to Y-6). For Y-5 and Y-6 samples before reaction, the V–O–V characteristic peak at 827 $cm^{-1}$ existed, and this is consistent with the $AgVO_3$ crystal phase given in the XRD analysis for these samples.

It can be concluded that the samples before reaction with the stretching vibration of vanadium–oxygen bond at 920 and 965 $cm^{-1}$ (see Fig. 1) showed very high selectivities for benzaldehyde (>20%). For Sample Y-4, these two absorption peaks were the strongest, and accordingly the selectivity for benzaldehyde was the highest. From the patterns of FT–IR samples after reaction (Fig. 2), it may be seen that the selectivity for benzaldehyde can be related to the change of the absorption peak site around 900 $cm^{-1}$. The wavenumber of the absorption peak of Sample Y-4 was the minimum (896 $cm^{-1}$), and the selectivity for benzaldehyde was the highest (57%). Therefore, it is concluded that the greater the red shift of FT–IR at about 900 $cm^{-1}$ for the samples after reaction, the weaker the strength of the V=O bond and the higher the selectivity for benzaldehyde.

(iii) *Measurements of ESR and TEM.* The ESR spectra of samples which have been reacted with the toluene/air mixture were obtained. The results showed that a broad peak of paramagnetic signal of $V^{4+}$ existed, and the *g*-factor measured was 1.97, which was in accordance with the references (*30–32*). The values of secondary integration of the $V^{4+}$ signal given in Table 4 were used to represent the relative quantities of $V^{4+}$ concentrations in samples. It is seen that the change of the $V^{4+}$ concentration of samples exhibited a volcanic shape curve with the increase of silver content in samples. From Table 4, it can also be seen that the $V^{4+}$ concentration of Sample Y-4 was the highest. As compared with the XRD results of Table 3, the content of $VO_2$ phase in Sample Y-4 was the least, and the contents of silver–vanadium phase ($Ag_{0.80}V_2O_5$ and $Ag_{0.68}V_2O_5$) were the highest. Since the $Ag_{0.80}V_2O_5$ could be expressed as $2Ag_2O \cdot 4VO_2 \cdot 3V_2O_5$ ($V^{4+}\% = 40$), and the $Ag_{0.68}V_2O_5$ could be expressed as $17\,Ag_2O \cdot 34VO_2 \cdot 33V_2O_5$ ($V^{4+}\% = 34$), it is clear that the $V^{4+}$ signals of ESR came from the $V^{4+}$ ions in the silver–vanadium oxide phase. When the selectivity for benzaldehyde shown in Table 1 is compared with the results of ESR analysis, it can also be seen that a good parallel relation exists between the selectivity for benzaldehyde and the $V^{4+}$ concentration in these samples.

Figures 4(a) and 4(b) are the TEM photomicrographs of Y-2 sample (V/Ag = 9/1) before reaction. The results of SMEA showed that the long-thin platelets in "A" position of Fig. 4(a) were the phase of $Ag_{0.35}V_2O_5\beta$, and the irregular plate-form crystal in "B" position of Fig 4(a) approached the composition of $AgV_7O_{18}$. The result of SMEA in the "C" position in Fig. 4(a) showed the atomic ratio of V/Ag to be 9.3. The electron diffraction indicated that it was a single crystal, and thus it could be ascribed to the silver entered into the $V_2O_5$ lattice to form solid solution. The "D" position in Fig. 4(b) was the phase of $AgV_7O_{18}$, and the "E" position in Fig. 4(b) was the pure vanadium, i.e., $V_2O_5$. Fig. 4(c) is the TEM photomicrograph of Sample Y-3 (V/Ag = 3/1) before reaction. The crystal size was larger as compared with Y-2 and Y-3 samples, and this result was consistent with the

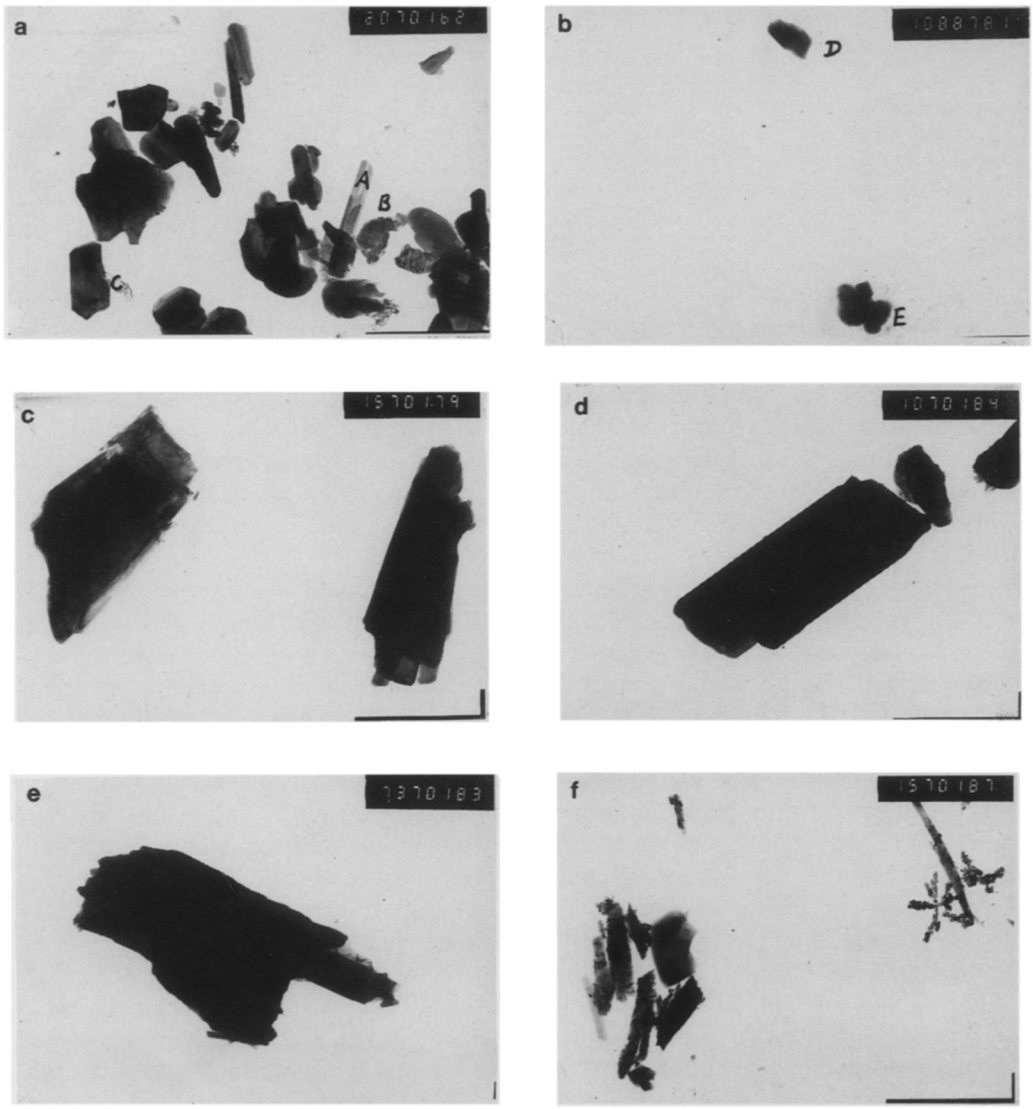


FIG. 4. TEM photomicrographs of V–Ag samples before reaction. (a) Y-2 (V/Ag = 9/1), 20000×; (b) Y-2 (V/Ag = 9–1), 10000×; (c) Y-3 (V/Ag = 3/1), 15000×; (d) Y-4 (V/Ag = 2.16), 10000×; (e) Y-4 (V/Ag = 2.16), 73000×; (f) Y-6 (V/Ag = 1/1), 15000×.

decrease of specific surface area in Table 1. The results of SMEA showed that the atomic ratio of V/Ag for the particle shown in Fig. 4(c) on the left was 2.5 and that shown in Fig. 4(c) on the right was 5.6, and the value of V/Ag was in accord with the value of V/Ag of the $Ag_{1\cdot2}V_3O_8$ phase and of the $Ag_{0\cdot35}V_2O_5\beta$ phase, respectively. In the TEM photomicrograph of Sample Y-4 (V/Ag = 2.16/1) before reaction, the measurement of SMEA showed that the composition of the large regular crystal (Fig. 4(d)) was 2.3 in V/Ag atomic ratio, the composition of the crystal in Fig. 4(e) was 2.5 in V/Ag atomic ratio, and the latter was consistent with a vanadium–silver atomic ratio of $Ag_{1\cdot2}V_3O_8$. Figure 4(f) is the TEM photomicrograph of Sample Y-6 (V/Ag = 1/1) be-

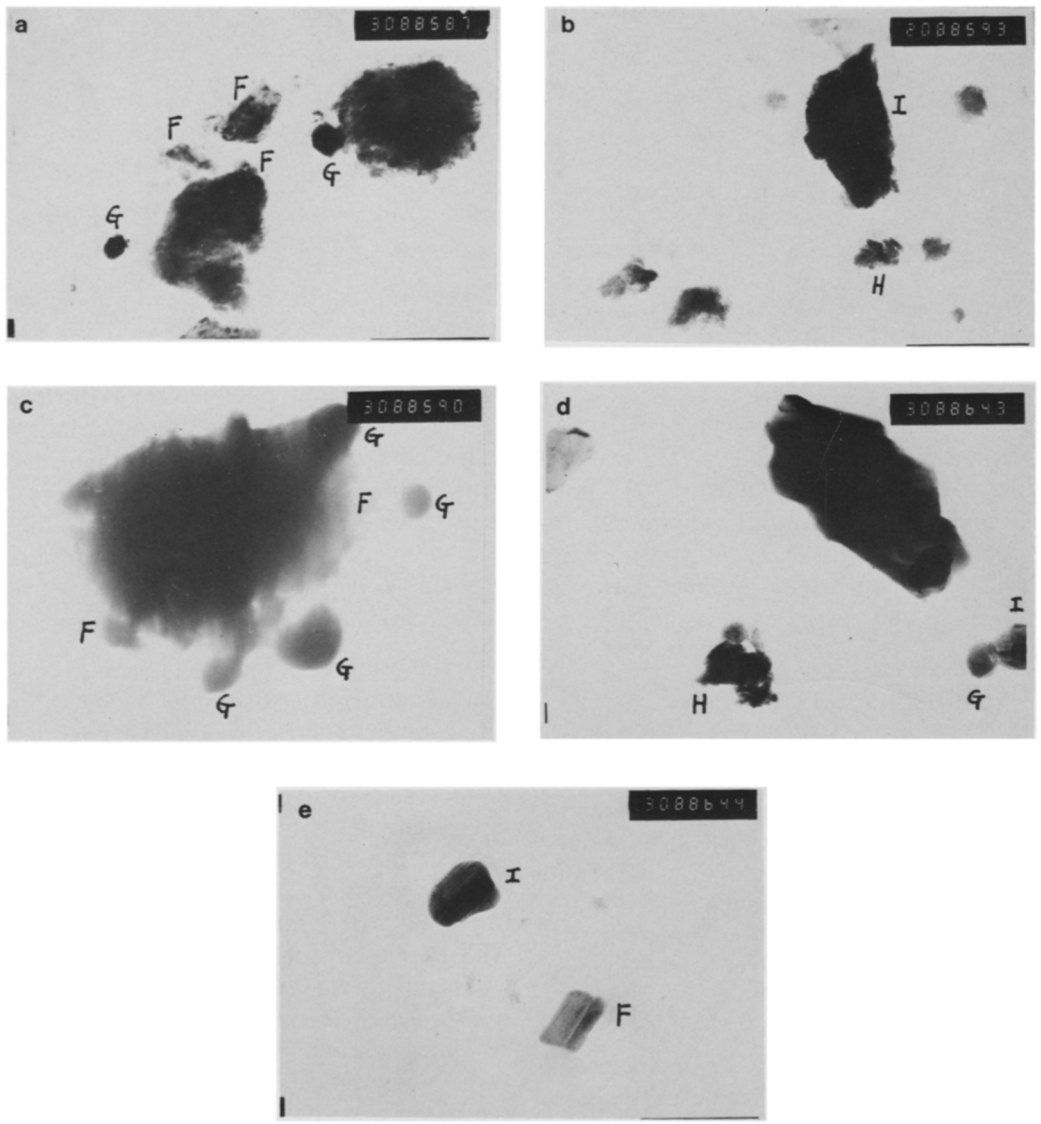


FIG. 5. TEM photomicrographs of V–Ag samples after reaction. (a) Y-2 (V/Ag = 9/1), 30000×; (b) Y-4 (V/Ag = 2.16), 20000×; (c) Y-4 (V/Ag = 2.16), 30000×; (d) Y-6 (V/Ag = 1/1), 30000×; (e) Y-6 (V/Ag = 1/1), 30000×.

fore reaction. The SMEA showed that the flower-branched crystal (on the right of Fig. 4(f) was metallic silver. The measurement of SMEA showed that the bar-like crystal on the left of the photograph had a V/Ag atomic ratio approaching 1.0, and this ratio can be regarded just as the value of V/Ag of the $AgVO_3$ crystal. Figure 5 shows the TEM photomicrographs of the three V–Ag samples of Y-2, Y-4 and Y-6 after reaction, and these photomicrographs are compared with those of V–Ag samples before reaction in Fig. 4. It can be seen that morphology and structure of the crystals had clear changes. The results of SMEA in Fig. 5 showed that the irregularly shaped crystal marked by "F" was vanadium, and when compared with the results of XRD (Table 3) these

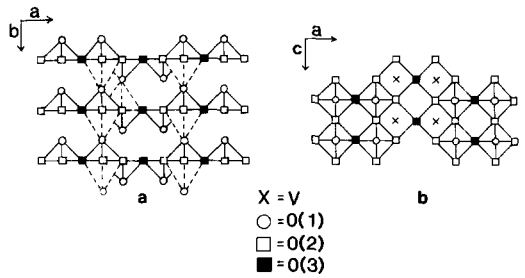


FIG. 6. Schematic presentation of the $V_2O_5$ structure. (a) (001) plane; (b) (010) plane.

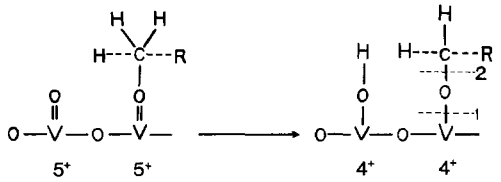


FIG. 7. Adsorption of toluene on $V_2O_5$. R-phenyl.

could be referred to as $V_2O_4$ or $VO_2$.The ball-shaped crystal marked by "G" was metallic silver. The V/Ag value of "H" position and "I" position in these photomicrographs is 2.53 and 2.95, and it was in accord with vanadium–silver atomic ratio of $Ag_{0.80}V_2O_5$ and $Ag_{0.682}V_2O_5$, respectively.

### 3. *Catalyst Structure and Catalytic Activity*

The structure of $V_2O_5$ is shown in Fig. 6 (*22*). It is generally accepted that for the $V_2O_5$ catalysts, the double bond oxygen of V–O(1) in the (010) plane plays an important role in the catalytic oxidation reaction, and that the activity of reaction is related to the strength of V=O bond (*33*). Kera *et al.* (*34*) have reported that the V=O bond takes part in the exchange of $O^{18}$ between $CO_2$ and $V_2O_5$, and they have also reported (*35*) that the oxygen exchange between the oxygen in gas phase and $V_2O_5$ occurred essentially on V=O bond. Niwa and Murakami (*36*) observed that, after toluene was adsorbed, the IR absorption peak which belongs to V=O at about 1000 $cm^{-1}$ disappeared. Maliński *et al.* (37) investigated the oxidation of methanol, and also obtained the same conclusion of V=O bond participating in the reaction. In the crystal of $V_2O_5$, a part of O(1) (see Fig. 6) which was connected with vanadium on the catalytically active (010) plane was probably absent at high temperatures during the catalytic oxidation. It is possible that the naked $V^{5+}$ ions on the (010) plane could act as adsorption sites for electron-donating species, so that the molecule of toluene existing on the surface of $V_2O_5$ could be dissociated from a hydrogen atom from the methyl radical first, and then act as the form of free radical adsorbed on the adjacent site of the catalyst surface. This mechanism is depicted in Fig. 7 (*21, 38*).

It is suggested that the oxidation of toluene molecules after activated adsorption probably occurs via the following three reaction paths:

(i) If the adsorbed toulene molecule is broken along the "1" position of V—O in Fig. 7 and another hydrogen was dissociated successively, then the reaction will result in a side-chain oxidation reaction to produce benzaldehyde.

(ii) If the adsorbed toluene molecule is broken along the "2" position of C—O bond in Fig. 7, the free redical of benzyl will react with the adsorbed toluene molecule on an adjacent site; therefore, the oxidation reaction proceeds along the oxidative coupling reaction path to give the reactive products.

(iii) When the adsorbed toluene molecule is reacted with the activated absorbed oxygen, it will give deep-oxidation products.

The above mentioned reaction paths of (i) and (ii) are the parallel competing reaction paths. Due to the fact that the catalytic capacity of the surface of the $V_2O_5$ sample for toluene is high (*17*), the possibility of reaction path (ii) of the oxidative reaction is the largest. Therefore, for the $V_2O_5$ catalyst (Y-1), the experiment has shown that the oxidative coupling prevails; there are quite a lot of oxidative coupling products, and the selectivity for benzaldehyde is very small.

With regard to the pure silver catalyst, a

great number of experimental facts showed that both molecular and atomic oxygen existed on the silver surface. Bradshaw *et al.* (*39*), using LEED, and Force and Bell (*40*), by adopting IR spectroscopy, demonstrated that $O^-$ existed on the surface of silver catalysts. Clarkson and McClellan (*41*) and Tanaka Yamashina (*42*), in turn by using the ESR method, demonstrated that $O_2^-$ existed on the surface of the silver catalyst. According to the investigation of thermodynamic stability, Bielański and Haber (*43*) suggested that the oxygen existed on the silver surface as a stable form of $O_2^-$ and $O^-$ species, but the dissolved oxygen in the bulk phase of silver catalyst existed as the atomic manner, and $O^-$ was more stable than $O_2^-$. Kobayashi *et al.* (*44*), using the transient response method, demonstrated that the dissolved oxygen in bulk phase had the capacity to oxidize ethylene to carbon dioxide and water.

Due to the fact that $O_2^-$ and $O^-$ ions are strong electrophilic reactants, they attack the sites of high charge density of reacted molecule, thus causing the carbonic framework to decompose and to form deep-oxidation products, and the results of activity measurement given in Table 1 demonstrate this point of view.

The measurements of temperature-programmed desorption mass spectra carried out in another experiment showed that after a small amount of silver was added to the vanadium pentoxide, the silver entered into the bulk phase of $V_2O_5$ but hardly had any effect on the bond property of the surface lattice oxygen, so that the catalytic activity of Sample Y-2 should approach that of Sample Y-1. During reaction, the oxidative coupling products were the essential species for Sample Y-2, and the selectivity for benzaldehyde improved only slightly (Table 1). Following the increase of the silver content in samples, the structure and property of the catalyst samples had an apparent change. Because the silver–vanadium oxide phase occurred in these samples, and the V=O bond was weakened (refer to the FT–IR

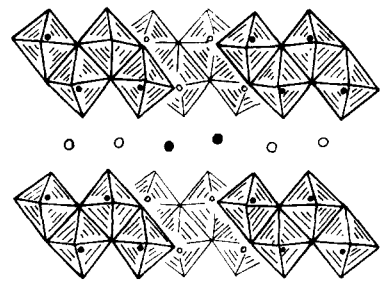

FIG. 8. The crystal structure of $Ag_{1-x}V_2O_5$. Large circles are silver atoms, small circles are vanadium atoms.

spectra), the specific activity of the catalysts increased. According to the results of XRD, it can be seen that the active phases of these samples after reaction were the silver–vanadium oxide phases ($Ag_{0.80}V_2O_5$ and $Ag_{0.68}V_2O_5$), whose structural scheme is given in Fig. 8, and the Ag–O bond lengths varied in the range of 2.48 Å to 2.68 Å (*45*). Because the silver–vanadium catalyst had two active sites, the activated toluene molecule reacted with the lattice oxygen to form the products of selective oxidation. Because the silver is the donor atom which has the strong capacity to give out electron, it promoted the capacity of converting the gaseous oxygen into the lattice oxygen, and resulted in the supplemental velocity of lattice oxygen and reoxidative velocity of $V^{4+}$ to proceed faster. Thus, the catalytic activity and selectivity of the samples greatly improved. For the V–Ag catalysts, when the content of silver arrived at a certain V/Ag ratio in the samples, it is favorable for the oxidative reaction to proceed along the reaction path (i). On the contrary, when the content of silver in samples is overabundant, the content of silver–vanadium oxide phases, $Ag_{0.80}V_2O_5$ and $Ag_{0.68}V_2O_5$, decreased and some elemental silver segregated, and therefore the selectivity for benzaldehyde decreased. So, it is concluded that over silver–vanadium oxide catalyst the oxidative reaction of toluene is carried out via the side-chain oxidation and oxidative cou-

pling reaction, which are the two parallel and competitive reaction paths. When the atomic ratio of vanadium–silver varies, the existing phases in these samples change, and this results in one of the two parallel and competitive reaction paths becoming depressed or promoted, thus causing the selectivity for benzaldehyde to increase or decrease. Because the identity of the intermediates which form in the selective oxidation of toluene to benzaldehyde and in the oxidative coupling reaction over the vanadium–silver catalyst are not known, and because more detailed information about how the structures of these catalysts change during reaction is needed, more advanced research should be carried out in this field.

## ACKNOWLEDGMENTS

The authors gratefully acknowledge the financial support from the Science Fund of Chinese Academy of Sciences, the Three Kinds Fund of the Nanjing University, and the Measured Fund of the Modern Analysis Centre of the Nanjing University.

## REFERENCES

1. van der Wiele, K., and van den Berg, P. J., *J. Catal.* **39,** 437 (1975).
2. Srivanstava, K. P., Madhok, K. L., and Jain, I. K., *India. J. Technol.* **18,** 135 (1980).
3. Nag, N. K., Fransen, T., and Mars, P., *J. Catal.* **68,** 77 (1981).
4. Madhok, K. L., and Srivastava, K. P., *Proc. Indian Acad. Sci. Chem. Sci.* **90,** 527 (1981).
5. Zhang, Hui-liang, Li, Zong-chang, and Fu, Xian-cai, *Cuihua Xuebao (Chinese Journal of Catalysis)* **9,** 331 (1988).
6. Zhang, Hui-liang, Li, Zong-chang, and Fu Xian-cai, *Cuihua Xuebao (Chinese Journal of Catalysis)* **9,** 339 (1988).
7. Zhang, Hui-liang, Li, Zong-chang, Fu, Xian-cai, Huang, Jian-ping, and Zhang, Yu-chang, *J. Mol. Catal. (China)* **3,** 139 (1989).
8. Jonson, B., Rebenstorf, B., Larsson, R., Andersson, S. L. T., and Lundin, S. T., *J. Chem. Soc., Faraday Trans. 1* **82,** 767 (1986).
9. Mori, K., Miyamoto, A., and Murakami, Y., *J. Chem. Soc. Faraday Trans. 1* **83,** 3303 (1987).
10. Jonson, B., Larsson, R., and Rebenstorf, B., *J. Catal.* **102,** 29 (1986).
11. Sharma, R. K., and Srivastava, R. D., *J. Catal* **65,** 481 (1980).
12. Ray, S. K., and Mukherjee, P. N., *Indian J. Technol.* **21,** 137 (1983).
13. Madhok, K. L., *React. Kinet. Catal. Lett.* **25,** 159 (1984).
14. Luo, Xiao-Ming, Chen, Ning, Chen, Yi, and Luo, Gu-feng, *Cuihua Xuebao (Chinese Journal of Catalysis)*, **9,** 351 (1988).
15. Ger. Offen., 2,730,761 (1978).
16. U.S.S.R., 495,301 (1975).
17. Wu,Yi-zu, and Wu, Zhi-nan, *Cuihua Xuebao (Chinese Journal of Catalysis)*, **4,** 210 (1983).
18. van den Berg, P. J., van der Wiele, K., and den Ridder, J. J. J., *in* "Proceedings, 8th International Congress on Catalysis, (Berlin 1984)," Vol. 5, P. 393. Dechema, Frankfurt-am-Main, 1984.
19. Casalot, A., and Pouchard, M., *Bull. Soc. Chim. Fr.* **10,** 3817 (1967).
20. Andersson, S. L. T., *J. Catal.* **98,** 138 (1986).
21. Andersson, A., and Lundin, S. T., *J. Catal.* **58,** 383 (1979).
22. Andersson, A., *J. Solid State Chem.* **42,** 263 (1982).
23. Frederickson, L. D., and Hausen, D. M., *Anal. Chem.* **35,** 818 (1963).
24. Koós, M., Hevesi, I., and Varga, A., *Acta Phys. Chem.* **19,** 29 (1973).
25. Andersson, A., Bovin, J. O., and Walter, P., *J. Catal.* **98,** 204 (1986).
26. Fikis, D. V., Heckley, K. W., Murphy, W. J., and Ross, R. A., *Canad. J. Chem.* **56,** 3078 (1978).
27. Tarama, K., Yoshida, S., Ishida, S., and Kakioka, H., *Bull. Chem. Soc. Jpn.*, **41,** 2840 (1968).
28. Andersson, A., *J. Catal.* **76,** 144 (1982).
29. Barraclough, C. G., Lewis, J., and Nyholm, R. S., *J. Chem. Soc.*, 3552 (1959).
30. Bielański, A., Dyrek, K., and Serwicka, E., *J. Catal.* **66,** 316 (1980).
31. Dyrek, K., and Łabanowska, M., *J. Catal.* **81,** 46 (1983).
32. Andersson, S. L. T., *J. Chem. Soc., Faraday Trans. 1* **82,** 1537 (1986).
33. Tarama, K., Teranishi, S., Yoshida, S., and Tamura, N., *in* "Proceedings, 3rd International Congress on Catalysis, Amsterdam, 1964," Vol. 1, 282. North-Holland, Amsterdam, 1965.
34. Kera, Y., Teratani, S., and Hirota, K., *Bull. Chem. Soc. Jpn.* **40,** 2458 (1967).
35. Kera, Y., and Hirota, K., *J. Phys. Chem.* **73,** 3973 (1969).
36. Niwa, M., and Murakami, Y., *J. Catal.* **76,** 9 (1982).
37. Maliński, R., Akimoto, M., and Echigoya, E., *J. Catal.* **44,** 101 (1976).
38. Andersson, S. L. T., and JäRås S., *J. Catal.* **64,** 51 (1980).
39. Bradshaw, A. M., Engelhardt, A., and Menzel, D., *Ber. Bunsenges Phys. Chem.* **76,** 500 (1972).
40. Force, E. L., and Bell, A. T., *J. Catal.* **40,** 356 (1975).

*41.* Clarkson, R. B., and McClellan, S., *J. Catal.* **61,** 551 (1980).
*42.* Tanaka, S., and Yamashina, T., *J. Catal.* **40,** 140 (1975).
*43.* Bielański, A., and Haber, J., *Catal. Rev.* **19,** 1 (1979).
*44.* Kobayashi, M., Yamamoto, M., and Kobayashi, H., *in* "Proceedings, 6th International Congress on Catalysis, London, 1976" (G. C. Bond, P. B. Wells, and F. C. Tompkins, Eds.), p. 336. The Chemical Society, London, 1976.
*45.* Andersson, S., *Acta Chem. Scand.* **19,** 1371 (1965).